A Novel Markov Random Field Segmentation Algorithm and Its Application to Breast Ultrasound Image Analysis

H. D. Cheng[1], Liming Hu[1], Jiawei Tian[2], and Litao Sun[2]

[1]Department of Computer Science, Utah State University, Logan, UT 84322 U.S.A.

[2]Second Affiliated Hospital of Harbin Medical University, Harbin, P. R. China

Abstract

Image segmentation is a vital step in image analysis, many segmentation algorithms have been developed. Markov random filed is successfully applied in this problem. In this paper, we propose a novel Markov random field segmentation algorithm based on the newly defined local energy, and implement it for breast ultrasound image analysis. Experiments demonstrate the proposed algorithm is less sensitive to noise than the traditional Metropolis sampler, and needs fewer iterations. It works well on the noisy breast ultrasound images.

Keywords: Markov Random Field, Gibbs distribution, Simulated Annealing, Gibbs Sampler, Metropolis sampler.

1. Introduction

Image segmentation is a process of dividing an image into separated regions, such that each region is homogeneous, but the joint of any two neighboring regions is inhomogeneous [1]. It is very essential and critical to image processing and pattern recognition. It is one of the most difficult tasks in image processing, and influences the final result of the image analysis.

Numerous segmentation methods have been studied in literature [1, 2]: edge-based methods, threshold methods, region-based methods. In this paper, we propose a grey level image segmentation based on Markov Random Field (MRF) approach, and apply this method to breast ultrasound image analysis.

MRF is a powerful stochastic tool to model the joint probability distribution of the image pixels considering the local spatial interactions [3, 4, 5]. MRF can be used in image restoration [6], image edge detection [7], image texture analysis and synthesis [8], and image segmentation: texture image segmentation [9], color image segmentation [10]. MRFs are also used in medical image analysis [11, 12, 13]. MRF attracts much more attention in the last 2 decades, there are a lot of research topics in MRF studies such as sampling methods [3, 4, 5], multiscale MRF [12], hierarchical multi resolution MRF [14, 15], and parameters estimation [16, 17]. MRFs are also combined with other approaches to model the image analysis problems, such as scale space [18], fuzzy logic [19], etc.

In the view of the random field, a segmentation process is a label process in the same lattice as the original image. The local spatial interaction relationship in the neighborhood can be integrated into a segmentation procedure. The distribution of an image includes the description of the dependence between local neighboring pixels, but not all models describing the local dependence are consistent with the global distribution of the image. A model is called Gibbs distribution, where its local models are consistent with the global model (MRF).

In this paper, we propose a novel MRF segmentation algorithm, and implement it for breast ultrasound image analysis. The improvements are: a) it is more robust to noise, even high level noise, b) the sampling algorithm needs fewer iterations to converge, and c) it works well with the noisy ultrasound images.

The paper is organized as follows: Section 2 introduces the MRF segmentation model, and discusses the proposed algorithm, Section 3 shows and explains the experimental results, and finally, Section 4 gives conclusions.

2. MRF Segmentation model

In the MRF image segmentation algorithm, we are interested in the following problem: giving a set of sites S={$s_{i,j}$| $1 \le i \le H$, $1 \le j \le W$}, and the observed grey level image, which can be represented as a one dimensional vector $Y = (y_{1,1}, y_{1,2}, \ldots, y_{i,j}, \ldots, y_{H*W})$, where H is the height of the image, and W is the width of the image, $y_{i,j} \in [0, 255]$ is the intensity of pixel $s_{i,j}$. After segmentation, we will get a labeled/segmented image $X= (x_{1,1}, x_{1,2}, \ldots, x_{i,j}, \ldots, x_{H*W})$, and $x_{i,j} \in [0, M-1]$, where M is the number of different labels, $x_{i,j} = m$ means the pixel at position $s_{i,j}$ ($s_{i,j} \in S$) of the original image has label m.

In the MRF, the most important concepts are the neighboring system and cliques. Fig. 1 describes the first order neighboring system and its cliques. As shown in Fig. 1(a), the site $s_{i,j}$ has 4 first-order neighbors ($s_{i-1,j}$, $s_{i+1,j}$, $s_{i,j-1}$, and $s_{i,j+1}$). Suppose the neighborhood set of $s_{i,j}$ is denoted as $\Box_{i,j}$ having 4 elements. Let $X_{|s_{i,j}}$ denote all the labels of image X except the label at site $s_{i,j}$, and $X_{\Box_{i,j}}$ denote the collection of neighboring pixels' labels around pixel $s_{i,j}$, then as a MRF, X has the following property: $P(x_{i,j} \mid X_{|s_{i,j}}) = P(x_{i,j} \mid X_{\Box_{i,j}})$, it states that the conditional distribution of $x_{i,j}$ under all the other pixels except $x_{i,j}$ is only dependent on its neighborhood system.

A clique C ($C \subseteq \Box_{i,j}$) is a subset of $\Box_{i,j}$ for which every pair of sites are neighbors. The single pixel $s_{i,j}$, is called single-pixel clique as an exception as shown in Fig. 1(b), and the cliques can also consist of the center pixel $s_{i,j}$ with another pixel in the neighborhood system called double-pixel clique, C_2, as shown in Fig. 1(c).

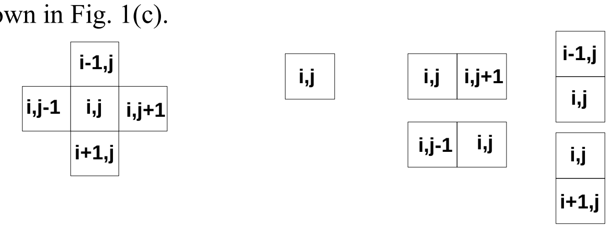

(a) (b) (c)

Figure 1. (a) the first order neighboring system of $s_{i,j}$; (b) single-pixel clique; (c) double-pixel cliques.

According to Hammersley-Clifford theorem [4], the probability of a random field X is given by a Gibbs distribution with respect to the neighboring system $N_{i,j}$:

$$P(X = x) = \frac{\exp(-U(x)/T)}{Z} \quad (1)$$

where x is a reality of MRF X, T is the temperature parameter, $Z = \sum_{x \in \Omega_X} \exp(-U(x)/T)$ is called normalizing constant or partition function, Ω_X is the set of all the possible realities of random field X, and U(x) is the energy function which can be written as:

$$U(x) = \sum_{x_{i,j} \in x} (V_1(x_{i,j}) + \sum_{\substack{(s_{i,j}, s_{i',j'}) \in C_2 \\ (i',j') \in \eta_{i,j}}} V_2(x_{i,j}, x_{i',j'}) \quad (2)$$

where $x \in \Omega_X$ is a reality of X, $x_{i,j}$ is a pixel of x, C_2 is the set of double-pixel cliques, $V_1(x_{i,j})$ is the potential function of the single-pixel clique $x_{i,j}$, $V_2(x_{i,j}, x_{i',j'})$ is the potential function of the double-pixel clique $(x_{i,j}, x_{i',j'})$, and U(x) is the energy function of the labeled image x.

The potential functions: V_1 $(x_{i,j})$ and $V_2(x_{i,j}, x_{i',j'})$ depend on the local configuration of the clique. For the double-pixel cliques, it is defined as:

$$V_2(x_{i,j}, x_{i',j'}) = \begin{cases} -\beta \text{ } if \text{ } x_{i,j} = x_{i',j'} \text{ and } (s_{i,j}, s_{i',j'}) \in C_2 \\ \beta \text{ } if \text{ } x_{i,j} \neq x_{i',j'} \text{ and } (s_{i,j}, s_{i',j'}) \in C_2 \end{cases} \quad (3)$$

Where β is a positive constant.

The potential function of single-pixel clique is defined as:

$$V_1(x_{i,j}) = \alpha_m \text{ if } x_{i,j} = m \quad (4)$$

where α_m is a constant associated with label m. The α_m 's are different only if the MRF is heterogeneous. Here, we consider that the MRF is homogeneous, and let $\alpha_m = \alpha$, m = 0… M-1.

The segmentation problem can be expressed in the Bayesian framework. According to Bayes' theorem:

$$P(X = x \mid Y = y) = \frac{P(Y = y \mid X = x)P(X = x)}{P(Y = y)} \quad (5)$$

where $P(X = x \mid Y = y)$ is the posteriori probability of $X = x$ conditioned on $Y = y$, $P(Y = y \mid X = x)$ denotes the probability distribution of $Y = y$ conditioned on $X = x$, $P(X = x)$ is a priori probability of $X = x$, and $P(Y = y)$ is the probability distribution of $Y = y$. What we are going to do is to maximize $P(X = x \mid Y = y)$ under the observed image Y=y (Maximize a Posterior). Under the observed image Y=y, $P(Y = y)$ can be disregarded, since it is a relative constant.

Let's assume $P(X = x \mid Y = y)$, $P(Y = y \mid X = x)$ and $P(X = x)$ are all Gibbs distributions and each component of Y=y in $P(Y = y \mid X = x)$ is independent on the other components with respect to X=x, then we will have:

$$U(x \mid y) = U(x) + U(y \mid x) \quad (6)$$

where $U(x \mid y)$, $U(x)$ and $U(y \mid x)$ are the corresponding energy functions of the Gibbs distribution. $U(x)$ is given by Eq. (2).

Another assumption is that the observed image Y=y under the condition of X=x is a Gaussian distribution with different means μ_m and variances σ_m^2, and based on the assumption of each component of Y=y in $P(Y = y \mid X = x)$ is independent on the other components with respect to X=x, then we will have:

$$p(y_{i,j} \mid x_{i,j} = m) = \frac{1}{\sqrt{(2\pi\sigma_m^2)}} \exp\left\{ -\frac{(y_{i,j} - \mu_m)^2}{2\sigma_m^2} \right\} \quad (7)$$

where (i,j) is the site $s_{i,j}$, m is the label of site $s_{i,j}$ in the segmented image x.

From Eq. (7), we will have:

$$U(y \mid x) = \sum_{i=1}^{H} \sum_{j=1}^{W} (\ln(\sqrt{2\pi}\sigma_m) + \frac{(y_{i,j} - \mu_m)^2}{2\sigma_m^2}) \quad (8)$$

where μ_m and σ_m^2 are the corresponding mean and variance of site $s_{i,j}$ in the observed image y, when pixel $s_{i,j}$ is labeled as m in the segmented image x.

So the objective of the MRF segmentation scheme is to assign a label to each pixel in the observed image y s. t. the energy function $U(x \mid y)$ is minimized, and it equals that x is the MAP estimator under the observed image y, that is:

$$\begin{aligned} \hat{x} &= \arg\max_{y \in \Omega_Y} P(X = x \mid Y = y) \\ &= \arg\max_{y \in \Omega_Y} (\frac{\exp(-U(x \mid y)/T)}{Z}) \\ &= \arg\min_{y \in \Omega_Y} U(x \mid y) \end{aligned} \quad (9)$$

where Ω_Y is the set of all possible configurations of y. Eq. (9) means the maximization of a posteriori conditional Gibbs distribution is equivalent to minimization of the energy of the model.

The energy function of the Gaussian MRF model is non-convex, we cannot get the global minimum by a deterministic algorithm (such as Iterated Conditional Modes (ICM) [3]), and it can only get the local minimum. Two classical sampling methods are used to meet the MAP criteria: The Metropolis sampler [5] and the Gibbs Sampler [4]. With a simulated annealing scheme, the Gibbs sampler and Metropolis sampler are guaranteed to convergence to the global minimum [4].

In our algorithm, we use the Metropolis Sampler, which works as follows:

(1) Set k = 0, assign a random initial configuration to x, and let $T=T_0$ be a sufficient high temperature. Here, we use K-Means algorithm [20] to initialize the segmented image, and we set T_0 =4.0 [4].

(2) Perturb the current configuration x_k to a new configuration x_{k+1} randomly, which differs at most in one pixel from the current configuration x_k, and calculate the energy $U(x_{k+1} \mid y)$ of the new configuration. We will scan the observed image y, line by line. For each pixel $s_{i,j}$, there are M possible labels, we totally have M possible new configurations which differs in one pixel from the current configuration, and the energy $U(x_k \mid y)$ of the old configuration, then get the energy difference:

$$\Delta U = U(x_{k+1} \mid y) - U(x_k \mid y) \quad (10)$$

and accept x_{k+1} if $\Delta U < 0$, else accept x_{k+1} with probability $\exp(-\frac{\Delta U}{T})$, that is:

$$x_k = \begin{cases} x_{k+1} & \text{if } \Delta U < 0 \\ x_{k+1} & \text{if } \Delta U \geq 0 \text{ and } \xi < \exp(-\dfrac{\Delta U}{T}) \\ x_k & \text{otherwise} \end{cases} \quad (11)$$

where $\xi \in [0,1)$ is a uniform random number.

(3) Decrease the temperature: T = T_{k+1} and goto step (2), until the system is in equibalance status. We use T_{k+1}=0.98*T_k, and judge if the system is in equibalance status by the global energy difference of two adjacent iterations, if the difference is less than 0.01, we say that the system is in equibalance status. One iteration means a scan of every pixel in the image.

We define the local energy of site $s_{i,j}$ as:

$$U_{local}(x_{i,j} \mid y_{\square_{i,j}}) = U(x_{i,j}) + U(y_{\square_{i,j}} \mid x) \quad (12)$$

Then ΔU can be written as:

$$\Delta U = U_{local}(x'_{i,j} \mid y_{\square_{i,j}}) - U_{local}(x_{i,j} \mid y_{\square_{i,j}}) \quad (13)$$

In the other words, when we scan the pixel $s_{i,j}$, if $x'_{i,j}$ is accepted as the new label of site $s_{i,j}$, depends only on the local energy of pixel $s_{i,j}$ under its neighboring system. It is assumed that the update of $x_{i,j}$ does not influence other pixels' local energy. This is how the traditional Metropolis sampler works.

In the above MRF image segmentation model, we notice that when we update $x_{i,j}$, we see that the double-pixel potentials of its 4 neighboring pixels also change. Under the first-order neighboring system, it only influences its 4-pixels' double-pixel potentials. In order to consider the influence of the update of $x_{i,j}$ on its 4-neighboring double-pixel potentials, we define the following local neighboring energy:

$$\begin{aligned} U_{\square-4}(x_{i,j}) &= U_{local}(x_{i,j} \mid y_{\square_{i,j}}) + U_{local}(x_{i-1,j} \mid y_{\square_{i-1,j}}) \\ &+ U_{local}(x_{i+1,j} \mid y_{\square_{i+1,j}}) + U_{local}(x_{i,j+1} \mid y_{\square_{i,j+1}}) \\ &+ U_{local}(x_{i,j-1} \mid y_{\square_{i,j-1}}) \end{aligned} \quad (14)$$

where $U_{local}(x_{i,j} \mid y_{\square_{i,j}})$, $U_{local}(x_{i-1,j} \mid y_{\square_{i-1,j}})$, $U_{local}(x_{i+1,j} \mid y_{\square_{i+1,j}})$, $U_{local}(x_{i,j+1} \mid y_{\square_{i,j+1}})$, $U_{local}(x_{i,j-1} \mid y_{\square_{i,j-1}})$ are the local energies of pixel $s_{i,j}$, and its 4 first order neighbors, $s_{i-1,j}$, $s_{i+1,j}$, $s_{i,j+1}$, $s_{i,j-1}$ are defined in Eq. (12).

Then ΔU can be represented as:

$$\Delta U = U_{\square-4}(x'_{i,j}) - U_{\square-4}(x_{i,j}) \quad (15)$$

Eq. (15) implies that when we scan the pixel $s_{i,j}$, whether $x'_{i,j}$ is accepted as the new label, depends not only on the local energy of pixel $s_{i,j}$ under its neighboring system, but also on the local energies of its 4 neighbors.

This new definition of local energy makes the system more consistent with the global model, and considers more on its neighboring system, therefore, it will be more tolerant to the noise, and needs fewer iterations to converge.

There are a few parameters need to be estimated in an unsupervised environment: Gaussian distribution parameters of each labels, such as mean μ_m and variance σ_m^2, and the total number of the labels, M.

Fortunately, the final results are not so sensitive to β, we will hold it as a constant, β=2.0, we suppose that the user knows how many segments in the image, and we will use the expectation-maximization (EM) algorithm [20] to estimate μ_m and σ_m^2. There are 2 main steps in the EM algorithm, it works as follows:

(1) Expectation or E-step: estimate μ_m and σ_m^2 of each label from the segmented image:

$$\mu_m = \frac{1}{N_m} \sum_{\substack{(i,j)\in S \\ x_{i,j}=m}} y_{i,j} \quad (16)$$

$$\sigma_m^2 = \frac{1}{N_m - 1} \sum_{\substack{(i,j)\in S \\ x_{i,j}=m}} (y_{i,j} - \mu_m)^2 \quad (17)$$

In Eq. (16) and Eq. (17), N_m is the number of pixels in image x that belong to label m.

(2) Maximization or M-step: use the estimated μ_m and σ_m^2 to refine the segmented image using the Metropolis sampler (do one iteration of step 2 and step 3 in the above Metropolis sampling algorithm).

(3) Repeat the above 2 steps until the system is in the equibalance status.

3. Experimental results

In order to demonstrate the performance of the proposed MRF segmentation algorithm, we have conducted a lot of experiments on the artificial images, and on the breast ultrasound images. Fig. 2(a) is a 4-class artificial image corrupted by additive Gaussian noise. From the histogram (Fig. 2(c)), we can see that most of threshold based segmentation algorithm will not work since there is no obvious valley in the histogram. Fig. 2(d) is the segmented image by k-means algorithm, as seen in this figure, this algorithm does not work, and the segmented image has a lot of noise; Fig. 2(e) is the segmented image by the Metropolis sampler after 112 iterations; Fig. 2(f) is the segmented image by the proposed algorithm after 98 iterations. The quality of these two segmented images is nearly the same, however, the proposed algorithm needs fewer iterations.

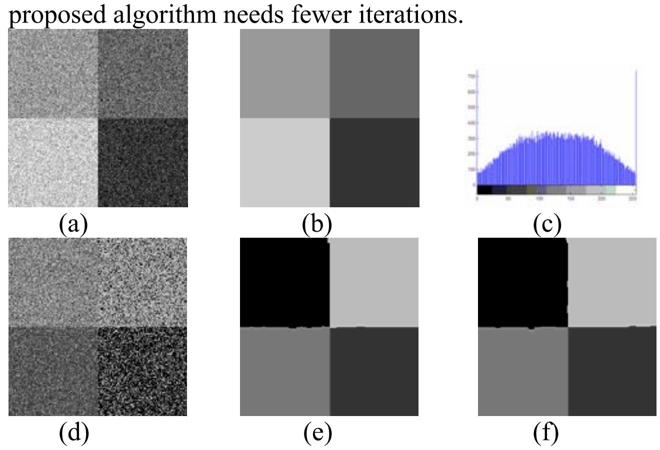

Figure 2. (a) original 4-class artificial image corrupted by additive Gaussian noise; (b) the original artificial image; (2) the histogram; (d) the segmented image by k-means algorithm; (e) the segmented image by Metropolis sampler; (f) the segmented image by the proposed algorithm.

We also applied the proposed algorithm to segment breast ultrasound images. The breast ultrasound images are obtained by an ultrasonic scanner (VIVID7) manufactured by GE Medical Systems, the frequency ranges of the ultrasonic scanner are: 5-12MHz. Because of the ultrasound's attenuation characteristics, same textures in different depths have different brightness, and the images are also corrupted by speckle noise. Fig. 3(a) is the original breast ultrasound image: most of the bright area are the background breast tissue, the suspected tumor area is corrupted by speckle noise, the first and most important step in breast ultrasound image analysis is to segment the suspected speckle-noised area from the background breast tissue in the depth attenuated environment; Fig. 3(b) is the segmented image by k-means algorithm, there are quite a lot of noises; Fig. 3(c) is the segmented image by Metropolis sampler after 267 iterations, this image is much better than the image in Fig. 3(b), but it still has some noises in the suspected area; Fig. 3(d) is the segmented image by the proposed algorithm after 247 iterations, as can be seen in the image, there are less noise in the image of Fig. 3(d), and the sampling algorithm needs fewer iterations. Further research on the combination of the proposed algorithm and fuzzy edge detector [21] will be investigated.

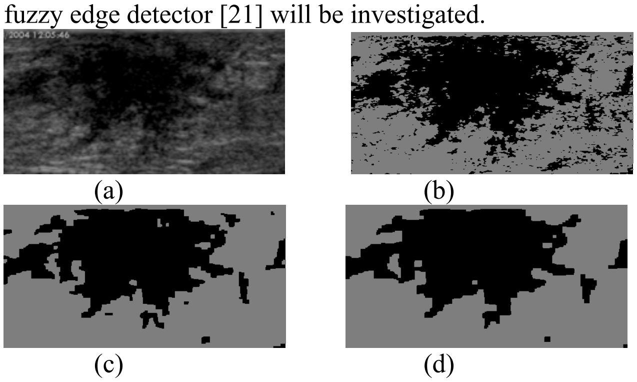

Figure 3. (a) the original breast ultrasound image; (b) the segmented image by k-means algorithm; (c) the segmented image by Metropolis sampler; (d) the segmented image by the proposed algorithm.

4. Conclusions

Image segmentation is a vital step in image analysis, many segmentation algorithms have been developed. MRF is successfully applied to such task. We developed an MRF segmentation algorithm based on the newly defined local energy. Experiments demonstrate the proposed algorithm is less sensitive to noise than the traditional Metropolis sampler, and needs fewer iterations, we also applied the proposed algorithm to breast ultrasound image analysis, the result is quite encouraging, and it works well with the noisy ultrasonic images.

5. References

[1] H. D. Cheng, X. H. Jiang, Y. Sun and Jing Li Wang, “Color Image Segmentation: Advances & Prospects”, *Pattern Recognition*, Vol.34, No.12, pp. 2259-2281, 2001.

[2] R. C. Gonzalez and R. E. Woods, “Digital Image Processing”, *second edition*, Pearson Education, Inc., 2002.

[3] J. E. Besag, “On the statistical analysis of dirty pictures”, *Journal of the Royal Statistical Society B*, Vol.48, No.3, pp. 259-302, 1986.

[4] S. Geman, and D. Geman, “Stochastic Relaxation, Gibbs Distributions, and the Bayesian Restoration of Images”, *IEEE Trans. on PAMI*, Vol.PAMI-6, No.6, pp. 721-741, 1984.

[5] M. Berthod, Z. Kato, S. Yu, J. Zerubia, “Bayesian image classification using Markov random fields”, *Image and Vision Computing*, No.14, pp. 285-295, 1996.

[6] D. Geman, and G. Reynolds, “Constrained Restoration and the Recovery of Discontinuities”, *IEEE Trans. on PAMI*, Vol.14, No.l3, pp.367-383, 1992.

[7] G. Winkler, V. Aurich, K. Hahn, A. Martin, and K. Rodenacker, “Noise Reduction in Images: Some Recent Edge-Preserving Methods”, *J. of Pattern Recognition and Image Analysis. Advances in Mathematical Theory and Applications*, Vol.9, No.4, pp. 749-766, 1999.

[8] R. Paget and I. D. Longstaff, “Texture synthesis via a noncausal nonparametric multiscale Markov random field”, *IEEE Trans. on Image Processing*, Vol.7, No.6, pp. 925-931, 1998.

[9] H. Derin, and H. Elliott, “Modeling and Segmentation of Noisy and Textured Images Using Gibbs Random Fields”, *IEEE Trans. on PAMI*, Vol.PAMI-9, No.1, pp. 39-55, 1987.

[10] H. Deng, and D. A. Clausi, “Unsupervised image segmentation using a simple MRF model with a new implementation scheme”, *Pattern Recognition*, Vol.37, No.12, pp.2323-2335, 2004.

[11] H.D. Li, M. Kallergi, L.P. Clarke, V.K. Jain, and R.A. Clark, “Markov Random Field for Tumor Detection in Digital Mammography”, *IEEE Trans. on Medical Imaging*, Vol.14, No.3, pp. 565-576, 1995.

[12] L. Zheng, and A.K. Chan, “An artificial intelligent algorithm for tumor detection in screening mammogram”, *IEEE Trans. on Medical Imaging*, Vol.20, No.7, pp. 559-567, 2001.

[13] A. Madabhushi, and D.N. Metaxas, “Combining Low-, High-Level and Empirical Domain Knowledge for Automated Segmentation of Ultrasonic Breast Lesions”, *IEEE Trans. on Medical Imaging*, Vol.22, No.3, pp.155-169, 2003.

[14] C.A. Bouman, and M. Shapiro, “A Multiscale Random Field Model for Bayesian Image Segmentation”, *IEEE Trans. on Image Processing*, Vol.3, No.2, pp.162-177, 1994.

[15] Z. Kato, T. C. Pong, and S. G. Qiang, “Unsupervised segmentation of color textured images using a multi-layer MRF model”, *ICIP03*, Vol. I, pp. 961-964.

[16] M.V. Ibánez, and A. Simó, “Parameter estimation in Markov random field image modeling with imperfect observations. A comparative study”, *Pattern Recognition Letters*, Vol.24, No.14, pp. 2377-2389, 2003.

[17] S. Lakshmanan, and H. Derin, “Simultaneous Parameter Estimation and Segmentation of Gibbs Random Fields Using Simulated Annealing”, *IEEE Trans. on PAMI*, Vol.11, No.8, pp.799-813, 1989.

[18] C. L. Huang, T. Y. Cheng, and C. C. Chen, “Color images' segmentation using scale space filter and Markov random field”, *Pattern Recognition*, Vol.25, No.10, pp. 1217-1229, 1992.

[19] S. Ruan, B. Moretti, J. Fadili, and D. Bloyet, “Segmentation of magnetic resonance images using fuzzy Markov random fields” *ICIP*, pp. 1051-1052, 2001.

[20] R. O. Duda, P. E. Hart and D. G. Stork, “Pattern Classification”, second edition, John Wiley & Sons, Inc, 2001.

[21] H. D. Cheng and Liming Hu, “A High Performance Edge Detector Based on Fuzzy Logic and Inference Rules”, submitted to *Digital Signal Processing*, 2004.